Title

Gene replacement in mice reveals that the heavily phosphorylated tail of neurofilament heavy subunit does not affect axonal caliber or the transit of cargoes in slow axonal transport.

Journal

The Journal of cell biology, 158(4)

ISSN

0021-9525

Authors

Rao, Mala V

Garcia, Michael L

Miyazaki, Yukio

et al.

Publication Date

2002-08-01

DOI

10.1083/jcb.200202037

Peer reviewed

JCB Article

Gene replacement in mice reveals that the heavily phosphorylated tail of neurofilament heavy subunit does not affect axonal caliber or the transit of cargoes in slow axonal transport

Mala V. Rao,[1,2] Michael L. Garcia,[4,5,6] Yukio Miyazaki,[4,5,6] Takahiro Gotow,[8] Aidong Yuan,[1] Salvatore Mattina,[1] Chris M. Ward,[4,5,6] Nigel A. Calcutt,[7] Yasuo Uchiyama,[9] Ralph A. Nixon,[1,2,3] and Don W. Cleveland[4,5,6]

[1]Nathan Kline Institute, [2]Department of Psychiatry, and [3]Department of Cell Biology, New York University School of Medicine, Orangeburg, NY 10962
[4]Ludwig Institute for Cancer Research, [5]Department of Cellular and Molecular Medicine, [6]Department of Neuroscience, and [7]Department of Pathology, University of California at San Diego, La Jolla, CA 92093
[8]Laboratory of Cell Biology, College of Nutrition, Koshien University, Hyogo 665-0006, Japan
[9]Department of Cell Biology and Neuroscience, Osaka University Graduate School of Medicine, Osaka 565-0871, Japan

The COOH-terminal tail of mammalian neurofilament heavy subunit (NF-H), the largest neurofilament subunit, contains 44-51 lysine–serine–proline repeats that are nearly stoichiometrically phosphorylated after assembly into neurofilaments in axons. Phosphorylation of these repeats has been implicated in promotion of radial growth of axons, control of nearest neighbor distances between neurofilaments or from neurofilaments to other structural components in axons, and as a determinant of slow axonal transport. These roles have now been tested through analysis of mice in which the NF-H gene was replaced by one deleted in the NF-H tail. Loss of the NF-H tail and all of its phosphorylation sites does not affect the number of neurofilaments, alter the ratios of the three neurofilament subunits, or affect the number of microtubules in axons. Additionally, it does not reduce interfilament spacing of most neurofilaments, the speed of action potential propagation, or mature cross-sectional areas of large motor or sensory axons, although its absence slows the speed of acquisition of normal diameters. Most surprisingly, at least in optic nerve axons, loss of the NF-H tail does not affect the rate of transport of neurofilament subunits.

Introduction

Neurofilaments (NFs),* the most abundant structural component of large myelinated axons, are obligate heteropolymers (Ching and Liem, 1993; Lee et al., 1993) composed of neurofilament heavy (NF-H, 200 kD), neurofilament medium (NF-M, 160 kD), and neurofilament light (NF-L, 68 kD) subunits. A series of experiments have implicated NFs in establishment of proper axonal diameters (Friede and Samorajski, 1970; Hoffman et al., 1987; Ohara et al., 1993; Xu et al., 1996; Zhu et al., 1997), itself a principal determinant of the velocity at which nerve impulses are propagated along axons (Gasser and Grundfest, 1939; Rushton, 1951; Waxman, 1980).

Earlier efforts with classical genetics, transgenic and gene-targeted mice have demonstrated that neurofilaments are essential for the establishment of normal axonal calibers. Absence (Ohara et al., 1993; Zhu et al., 1997) or strong reduction in axonal neurofilament numbers (Eyer and Peterson, 1994; Marszalek et al., 1996; Elder et al., 1998a; Jacomy et al., 1999) markedly suppresses the growth in axonal diameter that initiates during myelination. Simultaneous overexpression of NF-L and NF-M or NF-H increases overall radial growth (Xu et al., 1996; Meier et al., 1999), but the effect on caliber is sensitive to the ratio of the three neurofilament subunits as increases in any single subunit inhibit radial growth (Monteiro et al., 1990; Cote et al., 1993; Collard et

Address correspondence to Mala V. Rao, Nathan Kline Institute, 140 Old Orangeburg Rd., Orangeburg, NY 10962. Tel.: (845) 398-5547. Fax: (845) 398-5422. E-mail: rao@nki.rfmh.org

*Abbreviations used in this paper: KSP, lysine–serine–proline; mAb, monoclonal antibody; NF, neurofilament; NF-H, NF heavy; NF-L, NF light; NF-M, NF medium.

Key words: neurofilaments; NF-H phosphorylation; radial growth; axonal transport; conduction velocity

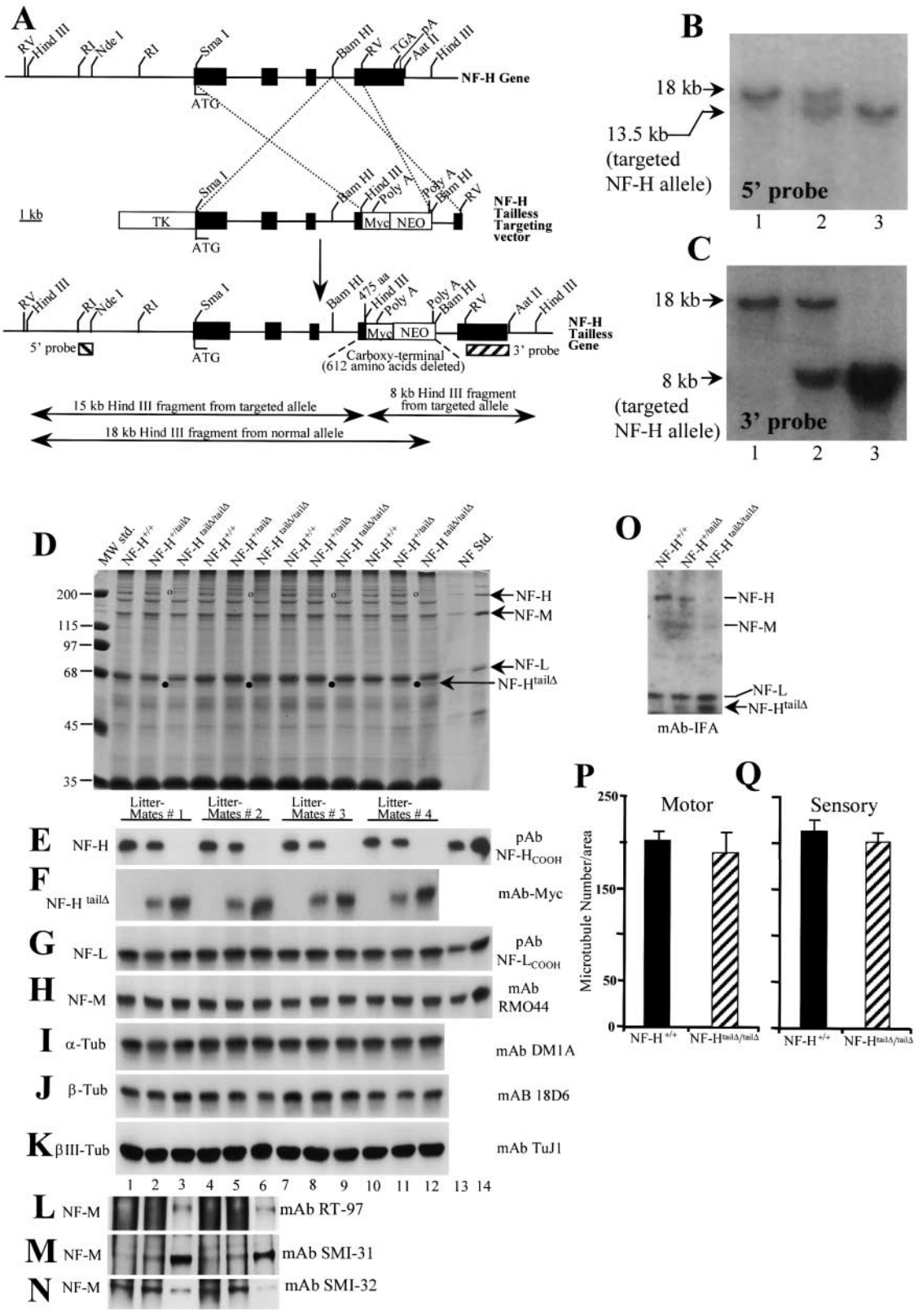

Figure 1. **Substitution of NF-H$^{tail\Delta}$ for wild-type NF-H does not affect stoichiometry of the neurofilament subunits.** (A) Construction of an NF-H$^{tail\Delta}$ allele in which the COOH-terminal 612 amino acids of the 660 amino acid tail of NF-H are replaced with a Myc epitope tag. The four exons of the NF-H gene are indicated by the filled boxes interrupted by three introns. ATG and TGA denote the translation initiation and termination codons. Dotted lines indicate the two regions where homologous recombination could take place between the targeting vector and the endogenous NF-H allele. (B and C) Screening of mouse tail DNAs for targeted deletion of NF-H tail. (B) Genomic DNA blots of mouse tails hybridized to the domain denoted as 5′ probe in A. (C) A similar blot as in B but hybridized with the sequence in A marked 3′ probe. DNAs are from littermate mice with (lane 1) two wild-type NF-H alleles, (lane 2) heterozygous, or (lane 3) homozygous for the NF-H$^{tail\Delta}$

al., 1995; Tu et al., 1995; Marszalek et al., 1996; Wong et al., 1996; Xu et al., 1996) even in the presence of higher numbers of axonal neurofilaments (Monteiro et al., 1990; Xu et al., 1996).

Several prior efforts have implicated phosphorylation of the NF-H tail as a regional influence on accumulation of neurofilaments, interfilament spacing and axonal calibers. The NF-M and NF-H subunits at steady state contain up to 15 and 50 moles of phosphate (Jones and Williams, 1982; Julien and Mushynski, 1982; Geisler et al., 1987; Goldstein et al., 1987; Lee et al., 1988), respectively, and are among the most extensively phosphorylated proteins in neurons (Julien and Mushynski, 1982, 1983; Carden et al., 1985). The COOH-terminal tail domains of NF-M and NF-H are phosphorylated at multiple lysine–serine–proline (KSP) repeat motifs. These phosphate groups appear on NF-M and NF-H only after they enter the axon (Sternberger and Sternberger, 1983; Lee et al., 1986; Glicksman et al., 1987; Oblinger et al., 1987; Nixon et al., 1987, 1990) and are metabolized relatively slowly compared to the NH_2-terminal phosphates (Nixon and Lewis, 1986; Sihag and Nixon, 1991). It has also been postulated that neurofilament behavior is regulated by complex events of phosphorylation (Nixon and Sihag, 1991; Nixon, 1993). NF-H tail phosphorylation has been closely linked to neurofilament-dependent control of axonal diameters (de Waegh et al., 1992; Hsieh et al., 1994; Nixon et al., 1994; Sanchez et al., 1996, 2000; Yin et al., 1998). One particularly persuasive finding used grafting of normal and myelination defective Schwann cells onto wild-type axons to demonstrate the presence of a signaling cascade from the myelinating cell to the axon (de Waegh et al., 1992). NF-H phosphorylation was markedly reduced in unmyelinated axonal segments, and this correlated with markedly reduced calibers, despite normal neurofilament content.

Axonal proteins are principally derived from those synthesized in the cell bodies and subsequently transported into the axon by slow and fast axonal transport mechanisms. Neurofilament, tubulin, and smaller amounts of fodrin and actin are transported as slow component a at the rate of 0.1–1 mm/day (Hoffman and Lasek, 1975; Black and Lasek, 1980). Other neuronal proteins advance as a slow component b at the rate of 2–20 mm/day, including more than 100 different proteins (e.g., actin, fodrin, myosin-like protein, clathrin, and many metabolic enzymes [Willard, 1977; Black and Lasek, 1979; Willard et al., 1979; Brady and Lasek, 1981; Garner and Lasek, 1981]). A longstanding controversy has been whether the neurofilament subunit proteins are transported as filaments, oligomers, or subunits (Terada et al., 1996; Bass and Brown, 1997; Hirokawa et al., 1997; Yabe et al., 1999; Prahlad et al., 2000; Roy et al., 2000; Shah et al., 2000; Wang et al., 2000; Shah and Cleveland, 2002).

As to the consequences of phosphorylation of the neurofilament tails, from observations in optic nerves it has been proposed that heavily phosphorylated NF-H subunits detach from the transport carrier and reside in the axon for months, whereas less phosphorylated variants are transported at normal slow axonal transport rates and have a short residence time in the axon (Lewis and Nixon, 1988). These observations have led to a model in which the COOH-terminal phosphorylation of neurofilament subunits regulates the interaction with a transport carrier and/or stationary axonal structures and thereby controls the rate of movement and residence time of neurofilaments within axons (Lewis and Nixon, 1988; Nixon and Sihag, 1991).

Consistent with this hypothesis is the finding that complete deletion of NF-H increases the rate of transport of the remaining neurofilament subunits in sciatic nerves (Zhu et al., 1998). Moreover, in cell culture studies in optic nerve axons, hypophosphorylated neurofilament subunits have been interpreted to undergo axonal transport more rapidly than subunits more extensively phosphorylated at their tail domains (Jung et al., 2000a), and the COOH-terminal phosphorylation of the NF-H subunit correlates with decreased neurofilament axonal transport velocity (Jung et al., 2000b, Yabe et al., 2001). Phosphorylation of KSP motifs triggered by a Schwann cell signal (see above) has been proposed as a key determinant of local control of neurofilament accumulation, interfilament spacing and radial growth of myelinated axons (de Waegh et al., 1992; Nixon et al., 1994; Sanchez et al., 1996, 2000; Yin et al., 1998).

To test these proposed in vivo functions of the NF-H subunit tail domain and its phosphorylation, we have now constructed NF-H tailless (NF-$H^{tail\Delta}$ mice by embryonic stem cell mediated gene knock in approach and analyzed the consequence of chronic loss of all 51 known phosphorylation sites on the murine NF-H subunit.

Results

Stoichiometric replacement of NF-H with an NF-H tailless subunit

To produce mice without the tail domain of NF-H (NF-$H^{tail\Delta}$), a gene targeting vector was constructed from the mouse NF-H gene in which the COOH-terminal 612 amino acids of NF-H were replaced with a Myc epitope tag and a neomycin phosphotransferase gene (Fig. 1 A). After electroporation, 2 out of 120 ES cell clones were identified to carry an NF-H gene allele correctly recombined into the

allele. (D–N) Loss of NF-H tail (and accumulation of NF-$H^{tail\Delta}$) has no effect on levels of NF-L, NF-M, or tubulin. Parallel immunoblots of sciatic nerve extracts from each of four sets of 3-mo-old wild-type, NF-$H^{tail\Delta}$ heterozygous and NF-$H^{tail\Delta}$ homozygous mice were fractionated on 7% SDS-polyacrylamide gels and stained with Coomassie blue (D) or immunoblotted (E–N) with antibodies that recognize: (E) NF-H in a phosphoin-dependent manner; (F) NF-$H^{tail\Delta}$ with Myc antibodies; (G) NF-L; (H) NF-M; (I) α tubulin; (J) β tubulin; and (K) neuron-specific β tubulin. (D, lanes 13 and 14) Quantification standards at right are provided by a twofold dilution series of a neurofilament preparation. Open (o) and closed dots mark the positions of NF-H and NF-$H^{tail\Delta}$ subunits, respectively. (L–N) NF-M phosphorylation levels in sciatic nerve extracts determined with three phosphorylation sensitive antibodies. (O) Measurement of the relative levels of accumulation of wild-type NF-H and NF-$H^{tail\Delta}$ using IFA (Pruss et al., 1981). (P and Q) Axonal microtubule density in motor (P) and sensory (Q) axons from L5 ventral or dorsal roots of wild-type or littermate homozygous NF-$H^{tail\Delta}$ mice. Density was measured by counting all microtubules in a given cross-sectional area. Counts are an average from 14 axons for each genotype of 6-mo-old animals.

NF-H gene. Both clones were injected into C57BL/6J blastocysts, producing chimeric animals that when bred to C57BL/6J mice transmitted the NF-H$^{tail\Delta}$ allele to their progeny. Mating pairs of mice heterozygous for the NF-H$^{tail\Delta}$ allele produced homozygous animals (Fig. 1, B and C, respectively) at the expected Mendelian frequency. These were viable and fertile, with no overt phenotype, up to 2 y of age.

Coomassie blue staining of sciatic nerve extracts revealed loss of full-length NF-H and appearance of a new polypeptide of 62 kD just below NF-L in NF-H$^{tail\Delta}$ homozygous animals (Fig. 1 D, lanes 6, 9, and 12). Immunoblotting with an antibody raised against the 13 COOH terminus amino acids of NF-H (Xu et al., 1993; pAb-NF-H$_{COOH}$) confirmed the absence of NF-H protein in sciatic nerve extracts of homozygous NF-H$^{tail\Delta}$ mice (Fig. 1, D and E). Heterozygous NF-H$^{tail\Delta}$ mice had 50–70% the normal level of full-length NF-H (Fig. 1 E, middle). With an antibody to its epitope tag, the NF-H$^{tail\Delta}$ subunit was confirmed to accumulate in a dose dependent manner (Fig. 1 F). Parallel immunoblots of sciatic nerve extracts revealed that NF-L (Fig. 1 G) and NF-M levels were unaffected by the absence of NF-H tails (Fig. 1 H).

To add further weight to the determination of the molar amounts of the NF-H$^{tail\Delta}$ subunit relative to the normal level of the full-length NF-H, we exploited monoclonal antibody IFA, which has been identified to bind to a conserved sequence element near the end of the helical domain of almost every intermediate filament subunit (Pruss et al., 1981; Geisler et al., 1983). This revealed an accumulated molar level for the NF-H$^{tail\Delta}$ subunit (at the expected 62 kD mobility) in NF-H$^{tail\Delta}$ homozygous mice that was similar to that for the full-length NF-H protein in wild-type nerve extracts (Fig. 1 O, compare lanes 1 and 3). This analysis also confirmed that there was no significant change in the levels of NF-L regardless of the presence or absence of the NF-H tails (Fig. 1 O). Identical results were found in analysis of optic nerve axons (unpublished data). Using two antibodies known to react with phosphorylated epitopes on NF-M (monoclonal antibody [mAb] RT97 and mAb SMI-31), in

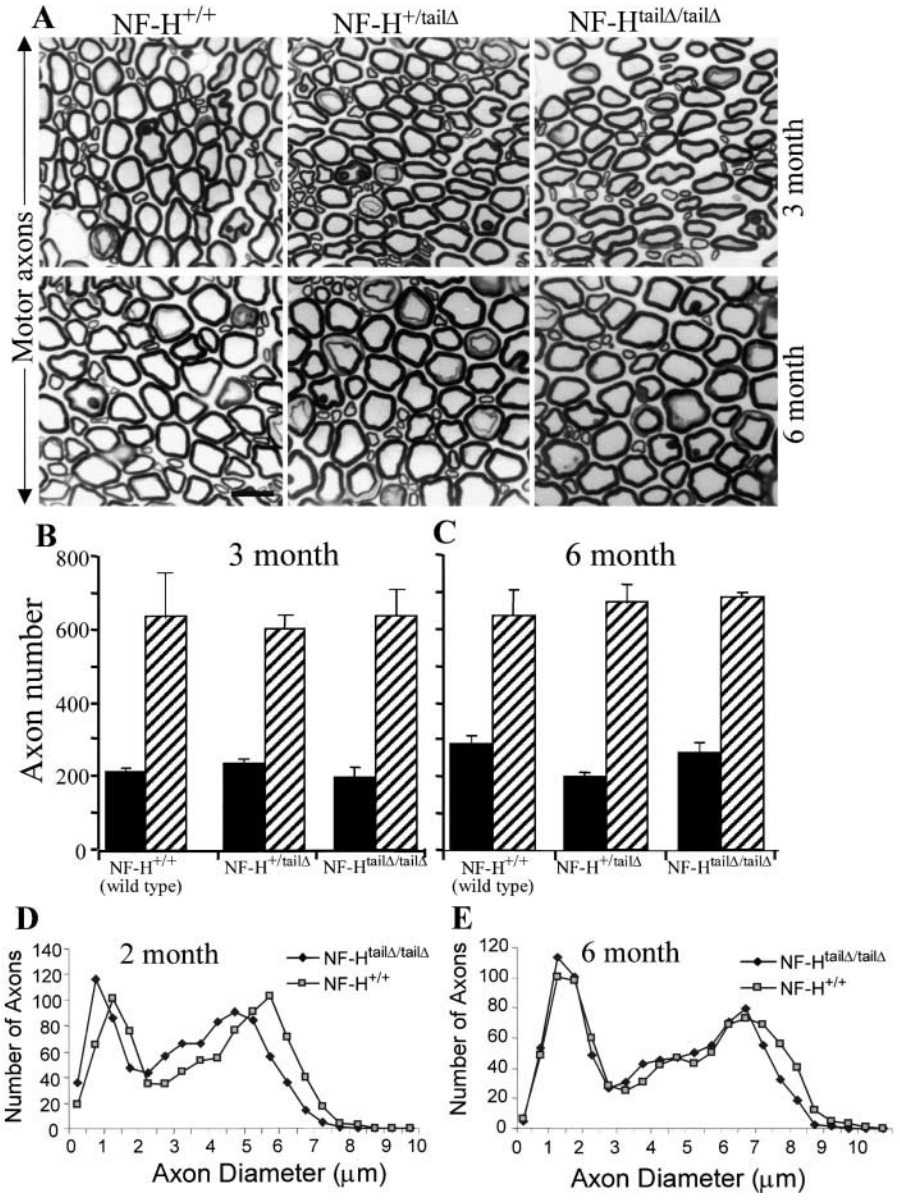

Figure 2. **Absence of NF-H tails does not markedly affect survival and radial growth of motor axons.** (A) Cross sections of L5 motor (ventral root) axonal profiles from wild-type, NF-H$^{tail\Delta}$ heterozygous and NF-H$^{tail\Delta}$ homozygous mice at 3 (top) or 6 mo (bottom) of age. Bar, 20 μm. (B and C) Numbers of small (<4 μm diameter, black bars) and large (>4 μm diameter, crosshatched bars) axons in L5 motor roots of 3- (B) or 6-mo-old (C) wild-type and NF-H$^{tail\Delta}$ heterozygous and homozygous mice. Counts are average from three to four animals for each genotype. (D–E) Distributions of axonal diameters in motor axons in 2- (D) or 6-mo-old (E) wild-type and NF-H$^{tail\Delta}$ heterozygous and homozygous animals. Points represent the averaged distribution of axon diameters from the entire roots of 5 mice for each genotype and age group.

the absence of NF-H tail it was found that NF-M was phosphorylated to a significantly higher level (Fig. 1, L and M) than in wild-type nerves, whereas unphosphorylated NF-M was diminished (Fig. 1 N).

Interactions between NF-H tails and tubulin do not affect axonal microtubule content

It has been proposed that NF-H tails specifically interact with the COOH-terminal region of β-tubulin and that this interaction may be regulated by τ protein kinase II (Miyasaka et al., 1993). Dephosphorylated neurofilaments have also been reported to bind more avidly to microtubules (Hisanaga and Hirokawa, 1990), and phosphorylation of the NF-H tail domain (by CDC2 kinase) has been shown to dissociate neurofilaments from microtubules in vitro (Hisanaga et al., 1991). When coupled with the earlier finding that deletion of NF-H leads to an elevation of tubulin content and number of axonal microtubules (Rao et al., 1998; Zhu et al., 1998), this raised the possibility that phosphorylation of the NF-H tail directly affects axonal microtubule content. However, examination of tubulin levels in the nerves of the NF-H$^{tail\Delta}$ mice revealed no change relative to wild-type mice in the axonal content of α-tubulin (Fig. 1 I), β-tubulin (Fig. 1 J), or the neuron-specific isoform β_{III}-tubulin (Fig. 1 K). This was confirmed by counting microtubule numbers in cross sections of motor or sensory axons from ventral or dorsal roots, respectively, from wild-type and littermate NF-H$^{tail\Delta}$ mice. Microtubule content was indistinguishable in both motor (Fig. 1 P) and sensory (Fig. 1 Q) axons. Thus, in contrast to earlier predictions, the heavily phosphorylated NF-H tails do not affect axonal microtubule content.

NF-H tails are not essential for the axonal growth of myelinated motor axons

In the absence of changes in NF-L and NF-M subunit levels (Fig. 1, G and H), the influence on radial axonal growth of the NF-H tail and its phosphorylation was examined by comparison of motor axons in the L5 ventral roots of ho-

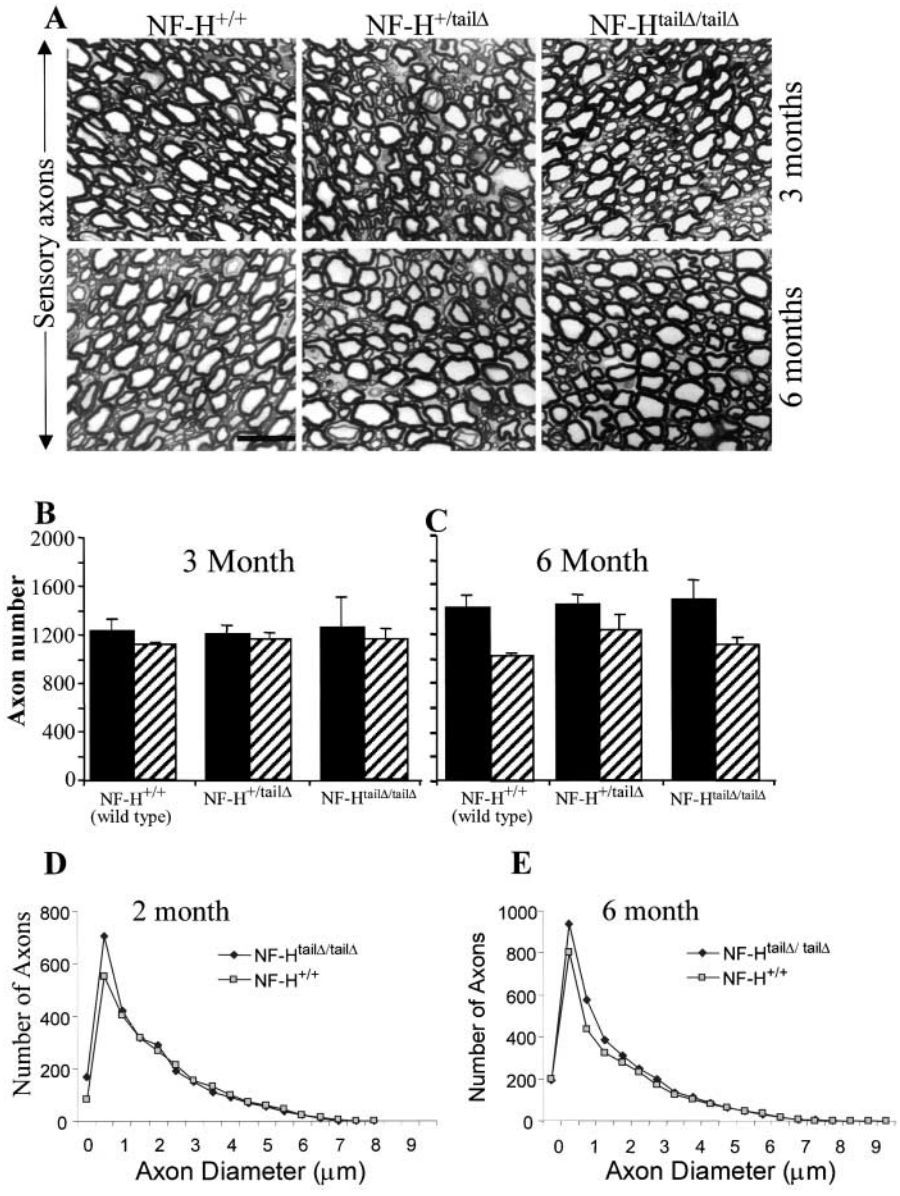

Figure 3. **Absence of NF-H tails does not alter caliber of sensory axons.** (A) Cross sections of L5 sensory (dorsal root) axonal profiles from wild-type, NF-H$^{tail\Delta}$ heterozygous and NF-H$^{tail\Delta}$ homozygous mice at 3 (top) or 6 mo (bottom) of age. Bar, 20 μm. (B and C) Numbers of small (<4 μm diameter, black bars) and large (>4 μm diameter, crosshatched bars) axons in L5 sensory roots of 3- (B) or 6-mo-old (C) wild-type and NF-H$^{tail\Delta}$ heterozygous and homozygous mice. Counts are average from three to four animals for each genotype. (D and E) Distributions of axonal diameters in sensory axons in 2- (D) or 6-mo-old (E) wild-type, NF-H$^{tail\Delta}$ heterozygous, and NF-H$^{tail\Delta}$ homozygous animals. Points represent the averaged distribution of axon diameters from the entire roots of five mice for each genotype and age group.

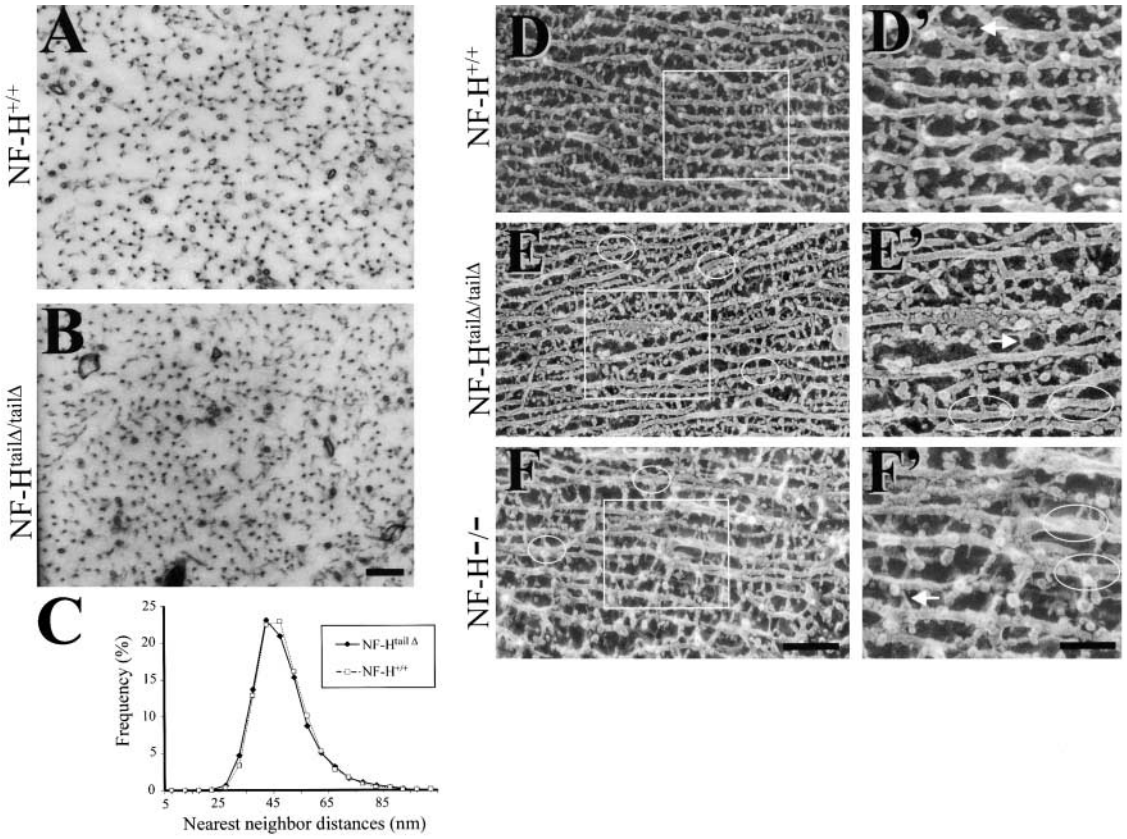

Figure 4. **Structure of axoplasm in the presence or absence of NF-H or its tail.** Thin-section electron micrographs of 3-mo-old motor axons of the L5 ventral roots of normal (A) or NF-H$^{tail\Delta}$ (B) animals. Bar, 400 nm. (C) Distributions of nearest neighbor distances from motor axons of 6-mo-old NF-H$^{tail\Delta}$ and wild-type mice. (D–F) Quick-freeze deep-etch micrographs of sciatic nerves from: (D) wild-type; (E) NF-H$^{tail\Delta}$; and (F) NF-H–null mice. Bar, 200 nm. (D′–F′) Higher magnification views of areas boxed in (D–F). Bar, 100 nm. Arrows point to plectin-like linkers. Ellipses highlight areas of closely apposed neurofilaments.

mozygous NF-H$^{tail\Delta}$ mice and their control littermates. Axonal profiles were found to be qualitatively indistinguishable (Fig. 2 A). To test this more precisely, cross-sectional areas of every axon within each ventral root (Fig. 2 A) were measured from 2- and 6-mo-old animals and effective diameters calculated from a circle of equivalent area. By 6 mo of age, wild-type and NF-H$^{tail\Delta}$ homozygotes displayed indistinguishable, bimodal distributions of axonal sizes, peaking at 1.5 and 6.5 μm (Fig. 2 E). Axon number in either size pool (as well as total number of axons) was not affected by absence of the NF-H tail (Fig. 2, B and C). Examination of younger animals revealed a possible slowing in the rate of growth of the largest axons in NF-H$^{tail\Delta}$ homozygotes (Fig. 2 D). These results demonstrate that without the confounding influences of compensatory changes in neurofilament number, NF-M content, and microtubules found when the entire NF-H subunit is deleted (Rao et al., 1998; Zhu et al., 1998), the NF-H tail, and phosphorylation of it, are not essential for neurofilament-dependent radial growth of motor axons (Fig. 2 E). However, at young ages it may affect the kinetics of growth of the largest axons (Fig. 2 D).

NF-H tails are not essential for the axonal growth of sensory axons

Loss of axonal NF-H in dorsal roots had previously been found to result in a loss of ~19% of sensory axons (Rao et al., 1998). To examine changes associated with the loss of NF-H tails on survival and calibers of sensory axons, axons of the L5 dorsal roots were counted and their diameters determined for wild-type and homozygous NF-H$^{tail\Delta}$ mice. No loss of either the smaller (<2 μm diameter) or larger (between 2 and 9 μm) caliber sensory axons (Fig. 3, B and C) was found in comparing the NF-H$^{tail\Delta}$ homozygotes with wild-type littermates. Although complete deletion of NF-H has been shown to slow caliber growth of the largest sensory axons (Rao et al., 1998), this was not found for the NF-H$^{tail\Delta}$ homozygotes at 2 (Fig. 3 D, two-tailed t test, $P > 0.16$) or 6 mo (Fig. 3 E). Thus, the NF-H tail and its multiple phosphorylation sites are neither the primary determinants of neurofilament-dependent radial growth of large myelinated sensory axons nor central to the ability of NF-H to stimulate survival of sensory axons in the first several months of postnatal development.

NF-H and its tails crossbridge between neurofilaments in vivo

To examine whether loss of the NF-H tail and its phosphorylation contributes to overall three dimensional organization of axoplasm, neurofilament and microtubule organization and interfilament distances were compared in cross-section electron micrographs of motor (Fig. 4, A and B) or sensory (unpublished data) axons. This revealed that the overall den-

sity (number/cross-sectional area) and general spatial distributions of neurofilaments and microtubules were not affected by absence of the NF-H tail, consistent with the unchanged content of tubulin and the three neurofilament subunits (Fig. 1). Inter-filament spacing was not significantly altered between NF-H$^{tail\Delta}$ axons (Fig. 4 B) and those from littermate controls (Fig. 4 A). Histograms of all interfilament distances from multiple axons from three 6-mo-old animals of each genotype were not distinguishable (Fig. 4 C; n = 55,000 and 49,000 for wild-type and NF-H$^{tail\Delta}$ motor axons, respectively). When considered with unaltered filament spacing after loss of the entirety of NF-H (Elder et al., 1998b; Rao et al., 1998), these findings imply that nearest neighbor distances are not primarily determined by NF-H (despite its ability to link adjacent neurofilaments [Chen et al., 2000]) or that such properties are shared with the NF-M tail or additional axonal components.

Long-range axonal organization was also examined in longitudinal axonal views using quick-freeze deep-etch electron microscopy of sciatic nerves from wild-type, NF-H deleted, or NF-H$^{tail\Delta}$ mice. Axoplasm of NF-H deleted (Fig. 4 F) or NF-H$^{tail\Delta}$ (Fig. 4 E) sciatic nerves was very similar to that of wild-type nerves (Fig. 4 D), with a few characteristic differences. The filaments and less abundant microtubules were generally oriented longitudinally within axoplasm (Fig. 4, D–F, compare NF-H$^{+/+}$ with NF-H$^{tail\Delta}$ or NF-H$^{-/-}$ deleted axoplasm), and interfilament distances were not significantly affected, with two exceptions. First, there were fewer crossbridges spanning between adjacent neurofilaments in either NF-H mutant (Fig. 4, E and F). Some of the remaining linkers between neurofilaments (Fig. 4, E and F, arrows) displayed the characteristic forked pattern of plectin (or plectin-related linkers) (Svitkina et al., 1996). Second, areas of close apposition of adjacent neurofilaments that were rarely seen in wild-type nerves were apparent in either NF-H mutant (Fig. 4, E and F, ellipsed areas). Although these comprised <1% of all nearest neighbor distances (i.e., a proportion too small to alter the overall distribution of distances; Fig. 4 C), their presence in the mice lacking the NF-H tail was consistent with a loss of a subset of crossbridging elements between adjacent neurofilaments.

NF-H tails do not affect the slow axonal transport

Extensive data from optic nerve (Nixon et al., 1982, 1987, 1994; Lewis and Nixon, 1988; Nixon and Sihag, 1991) and cell culture studies (Jung et al., 2000a, 2000b; Yabe et al., 2001) have implicated phosphorylation of NF-H and NF-M tails in age-dependent slowing of neurofilament transport rates within axons. This has led to the proposal that less phosphorylated species of NF-H are transported at a much faster rate(s) than more phosphorylated forms (Lewis and Nixon, 1988; Jung et al., 2000a, 2000b). Collectively, these observations have fueled the hypothesis that NF-H COOH-terminal phosphorylation and subsequent crossbridges from neurofilament to neurofilament are responsible for slowing neurofilament axonal transport, especially in optic nerves (Nixon et al., 1982, 1987, 1994; Lewis and Nixon, 1988; Nixon and Sihag, 1991).

To test this model, the rate of slow axonal transport of neurofilaments was determined in optic nerves of wild-type, NF-H deleted, or NF-H$^{tail\Delta}$ mice. After intravitreal injection of ^{35}S-methionine into an eye, slow axonal transport components were visualized by removal of the optic nerve 7 d postinjection, homogenization of 1.1-mm segments and visualized by gel electrophoresis and phosphorimaging (Fig. 5, A–D). This revealed that neither the complete absence of NF-H (Fig. 5, A and B and quantified in E–G) nor the deletion of its tail (Fig. 6, compare A and B, quantified in E–G) affected rate of transport of the remaining two neurofilament subunits NF-M and NF-L, relative to their rates in wild-type axons. Similarly, there was no difference in the rate of transport of cytoskeletal (Figs. 5, H and I and 6, H and I) or soluble (Figs. 5, compare C and D, quantified in J and K, and 6, J and K) tubulin and actin. In the NF-H$^{tail\Delta}$ mice, the 62-kD NF-H$^{tail\Delta}$ subunit appeared as a new cargo (Fig. 6 B) transported at a net velocity indistinguishable from that of NF-H in wild-type nerves.

Loss of NF-H tails does not influence the propagation of electric impulses along the nerve

An earlier report found a reduced axonal conduction velocity in mice deleted in NF-H (Zhu et al., 1998) despite no significant loss in axonal diameter or myelination. To test whether the loss of the NF-H tail and its influence on axoplasmic structure also affected axonal conduction, velocity of transmission was measured in motor axons of sciatic nerves from 5-mo-old wild-type, NF-H$^{tail\Delta}$, and NF-H deleted mice (Table I). As found previously, velocity in NF-H deleted mice was reduced by 30% relative to wild-type mice (36.4 ± 0.9 m/s for NF-H$^{-/-}$ vs. 52.2 ± 1.9 m/s for wild-type). However, conduction velocity in 5-mo-old mice was not decreased in NF-H$^{tail\Delta}$ mice (53.6 ± 1.2 m/s).

Discussion

The developing mammalian nervous system undergoes two phases of growth. Axons first extend from their point of origin to their targets where they form stable synapses. Subsequently, and concomitant with myelin formation, axons undergo a rapid phase of radial growth. This large increase in axonal volume is essential for basic neuronal properties such as rates of nerve conduction. Alterations in expression after sciatic nerve injury initially implicated a role for neurofilaments in establishing the diameter of large myelinated fibers (Hoffman et al., 1987). Genetics unequivocally established this role for neurofilaments: radial growth is severely compromised by absence of neurofilaments resulting from gene mutation (Ohara et al., 1993) or deletion (Zhu et al., 1997). Radial growth is

Table I. **Absence of NF-H, but not its tail, slows nerve conduction velocity**

Genotype	Conduction velocity
	(m/s) ± SEM
NF-H$^{+/+}$	52.2 ± 1.95
NF-H$^{tail\Delta/tail\Delta}$	53.6 ± 1.19
NF-H$^{-/-}$	36.4 ± 0.949

Nerve conduction velocity measurements were performed on motor axons in the sciatic nerve from control, NF-H$^{tail\Delta}$, and NF-H$^{-/-}$ mice. Values shown are from a minimum of five animals for each genotype, and the recordings are done in triplicate for each animal.

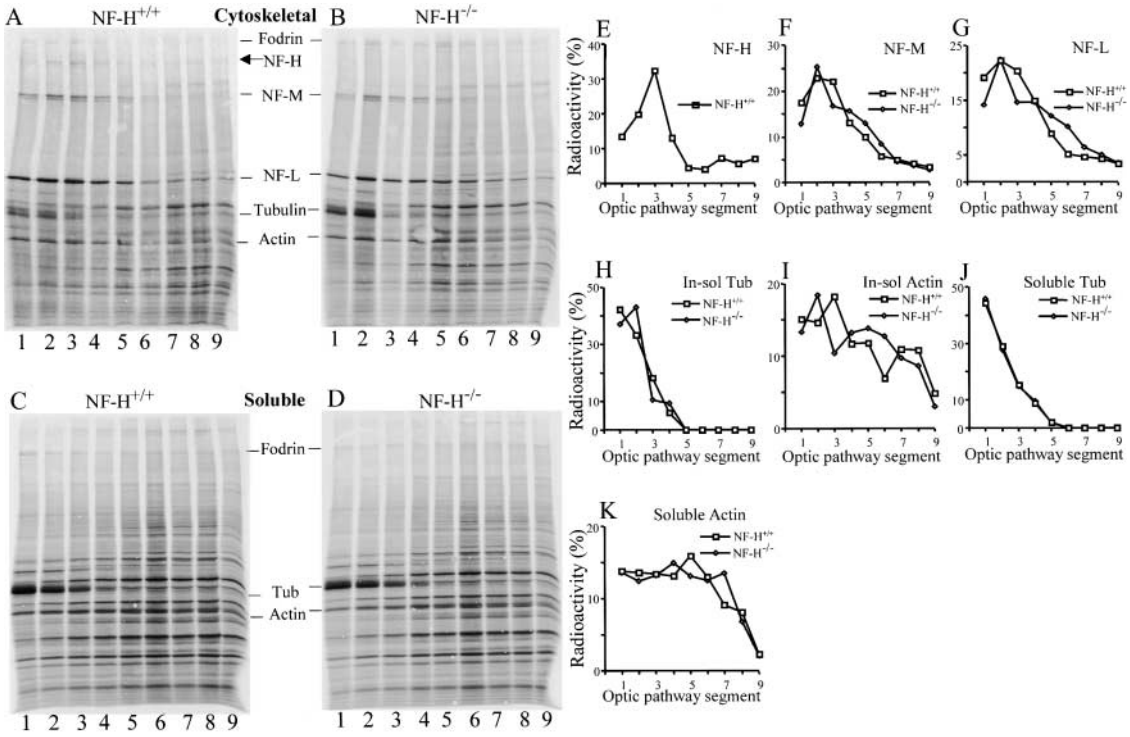

Figure 5. **The NF-H subunit does not slow transport in optic nerve.** (A–D) The speed and composition of slow axonal transport was determined by intravitreal injection of radiolabeled ^{35}S-methionine into 3-mo-old control (A and C) and NF-H–deleted (B and D) mice. Optic nerve proteins were fractionated into cytoskeleton (A and B) and soluble fractions (C and D) with a Triton X-100–containing buffer. Fractionated proteins were separated on 5–15% SDS-polyacrylamide gels, transferred to nitrocellulose, and visualized by x-ray film and phosphorimaging. (E–K) Quantification of NF subunits, tubulin, and actin transport in optic nerves. (E) NF-H; (F) NF-M; (G) NF-L; (H) cytoskeletal tubulin; (I) cytoskeletal actin; (J) soluble tubulin; and (K) soluble actin.

also dependent on signaling to the axons by myelinating cells, as demonstrated conclusively by loss of caliber in axonal segments ensheathed by myelin defective Schwann cells (de Waegh et al., 1992; Sanchez et al., 1996). The presence of functional myelin triggers a cascade of neurofilament phosphorylation (or inhibition of phosphatase action or both) leading to axonal expansion in myelinated internodes and absence of such growth in the initial unmyelinated axonal segment and unmyelinated nodes (Hsieh et al., 1994). Moreover, radial growth is correlated with the nearly stoichiometric phosphorylation of the NF-H tail (Julien and Mushynski, 1983; Carden et al., 1985; Lee et al., 1988).

A possible explanation for radial growth being associated with phosphorylation of NF-H is that phosphorylation is linked with a reduction in the rate of slow axonal transport, possibly allowing phosphorylated neurofilaments to incorporate into the existing cytoskeletal network (Nixon et al., 1982, 1987, 1994; Lewis and Nixon, 1988; Nixon and Sihag, 1991; Yin et al., 1998; Jung et al., 2000a, 2000b; Sanchez et al., 2000; Yabe et al., 2001). Consistent with these observations, deletion of NF-H subunit yielded decreased survival and reduced radial growth in the largest sensory axons (Rao et al., 1998). Therefore, it seemed reasonable to predict that the tail domain of NF-H, with its 51 potential phosphorylation sites, is required for survival and radial growth of sensory axons. However, our evidence here demonstrates that this cannot be so. A primary contributor to radial growth cannot simply be phosphorylation of the NF-H tail, as loss of all phosphorylation sites, without compensatory changes in other major cytoskeletal components, does not compromise survival or caliber development.

However, the organization of axoplasm in NF-H$^{tail\Delta}$ mice is subtly altered: there is reduction in the density of projections from the core of each neurofilament and an increased frequency in neurofilaments that longitudinally contact each other for distances of up to 300 nm (Fig. 4 E). This is as expected if the NF-H tail is a major linker that combines with others to set a spacing of ~40 nm between filaments. From stochastic considerations, without NF-H, the reduction in overall linkers would be expected to yield close apposition of filaments, depending on how many such linkers were required or available per unit length of filament. Although, the nearest neighbor filament spacing is not significantly affected by the loss of NF-H tail, again as expected if other crossbridgers were still present, such as NF-M that could establish a similar spacing. In any event, our evidence indicates that the overall composition of the neurofilament network contributes much more to axonal survival and maturation than does the NF-H tail and its phosphorylation.

Earlier biochemical evidence supported an influence of the NF-H tail, but not the NF-M tail, on tubulin subunits as a function of the phosphorylation state of NF-H. Such an interaction has been proposed to be controlled by τ associated protein kinase II and CDC2 like kinase (Hisanaga and Hirokawa, 1990; Hisanaga et al., 1991; Miyasaka et al., 1993). Indeed, the loss of the entire NF-H subunit yields elevated levels of microtubules in sciatic nerves (Rao et al., 1998; Zhu et al., 1998). However, loss of NF-H tails in NF-H$^{tail\Delta}$ mice

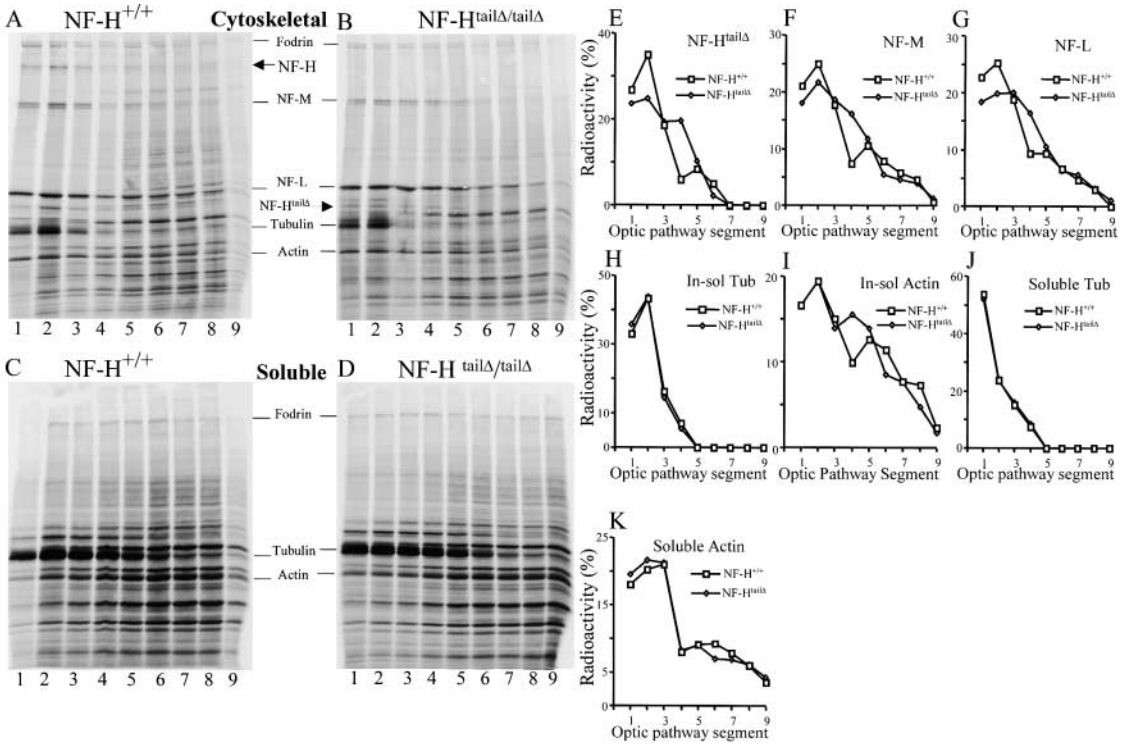

Figure 6. **Absence of the NF-H tail and its phosphorylation does not affect the rate or composition of slow axonal transport in optic axons.** (A–D) Slow axonal transport was measured as noted in the legend to Fig. 5, except using wild-type (A and C) or (B and D) NF-H$^{tail\Delta}$ mice.

did not yield an increase in either total tubulin or microtubule density in axons (or levels or speed of tubulin transport), from which we conclude that in vivo the heavily phosphorylated NF-H tail does not contribute significantly to microtubule content or organization in the axon.

Neurofilament phosphorylation has also been closely linked to the rate of slow axonal transport in optic nerves and cell culture models (Nixon et al., 1982, 1987, 1994; Lewis and Nixon, 1988; Nixon and Sihag, 1991; Yin et al., 1998; Jung et al., 2000a, 2000b; Sanchez et al., 2000; Yabe et al., 2001). Moreover, it has long been proposed that incorporation of the NF-H subunit slows the speed of slow axonal transport (Willard and Simon, 1983). Consistent with this, less phosphorylated species of NF-H are transported at a much faster rate than more phosphorylated forms (Lewis and Nixon, 1988; Jung et al., 2000a, 2000b). Repetitive phosphorylation of the COOH-terminal tail of NF-H has thus seemed a reasonable mechanism to modulate slow transport rates. However, our evidence here does not offer confirmation of this hypothesis. In optic nerve axons, COOH-terminal truncation, resulting in complete loss of all potential tail domain phosphorylation sites, does not affect slow transport rates (Fig. 6). Additionally, previous evidence had indicated that slow transport rates of about half the neurofilament subunits within motor axons of the sciatic nerve are accelerated by complete removal of NF-H (Zhu et al., 1998), with a corresponding increase in NF-M content and microtubules (Rao et al., 1998; Zhu et al., 1998). Conversely, increased expression of NF-H is associated with slowed rates of neurofilament transport (Collard et al., 1995; Marszalek et al., 1996). Because the subunit stoichiometry of neurofilaments is not altered by truncating the NF-H tail (Fig. 1), it might be predicted that slow transport rates within the sciatic nerve of the NF-H$^{tail\Delta}$ mice would remain unchanged relative to wild-type mice. A direct test of this is now underway.

Both NF-H deletion (Rao et al., 1998) and COOH-terminal truncation (Fig. 2 D) retarded the initial rate of radial growth of motor neurons, although by 6 mo wild-type axon diameters were achieved. For the NF-H$^{tail\Delta}$ mice, such slowing of radial growth cannot be explained by compensatory changes in other members of the neurofilament gene family or other known cytoskeletal components. Presumably, the volume determining axonal scaffold, of which neurofilaments are one important component, is assembled with at least partially redundant linkers. Thus, absence of the crossbridges from the NF-H tail kinetically delays, but does not preclude, establishment of a fully functional three-dimensional filament array.

Slowed radial growth offers an explanation for the otherwise unexpected reduction in conduction velocity in motor axons of the NF-H deleted mice, despite little effect on diameters measured in the motor roots. An initial proposal for the reduced velocity was a possible NF-H–dependent effect on the clustering of K^+ channels at nodes (Kriz et al., 2000). It seems to us much more likely that the significant loss of conduction velocity arises from a slowed propagation in radial growth distally along the nerves. For peripheral motor neurons, radial growth measurements can only be sampled in motor roots, that is, at a position within the first 5% of the length along these long axons (well before sensory and motor axons intermingle to form mature nerves). However, motor conduction velocities are measured much more distally in the nerve segment. Thus, in the absence of NF-H (and in the

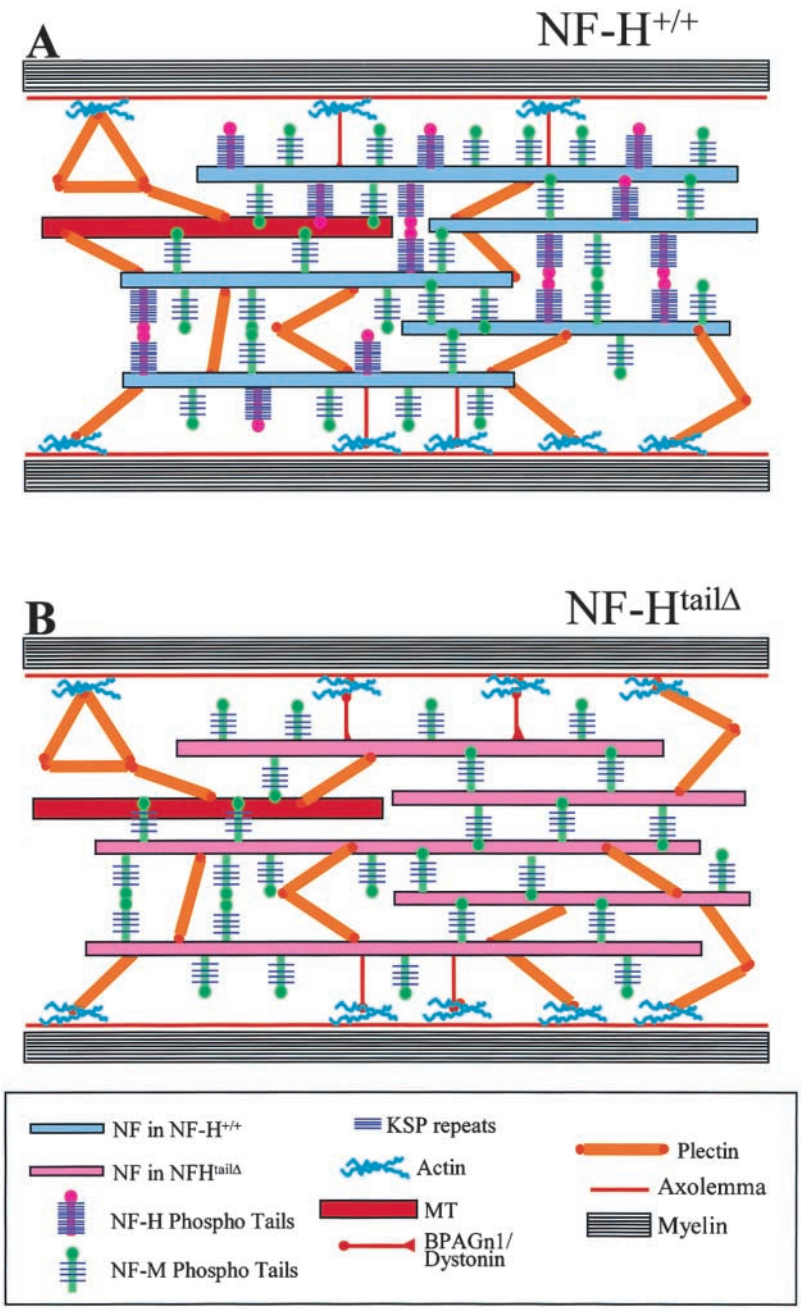

Figure 7. **Model of neurofilament dependent structuring of axoplasm.** In normal axons (A), axoplasm is organized into a volume-determining three-dimensional array by a series of linkages that span between adjacent neurofilaments (blue-gray) and between neurofilament and microtubules (red) or cortical actin (blue) filaments. NF-M (turquoise) and NF-H tails (purple) form crossbridges between neurofilaments (Nakagawa et al., 1995; Chen et al., 2000). Neurofilaments, microtubules, and cortical actin are interlinked by plectin and/or plectin-like linkers (orange) (Wiche, 1989; Errante et al., 1994; Svitkina et al., 1996). The neuronal cytoskeleton is also stabilized by the additional linkage of plakin family crosslinker proteins (BPAGn/dystonin/Acf7/MACF) between neurofilaments, microtubules, and actin in motor and sensory axons (Yang et al., 1996; Dalpe et al., 1998; Leung et al., 1999, 2001; Bernier et al., 2000). (B) In absence of NF-H tails, NF-M and other linkers (plectin, BPAGn/dystonin/Acf7/MACF, gigaxonin) continue to support a three-dimensional array essential for support and maintenance of normal axonal volume.

presence of the accompanying elevation in microtubules and NF-M), the simplest view is that growth in caliber is retarded both proximally (as we have measured in motor roots of 2-mo-old animals) and along most of the length of sciatic nerve axons (as we have measured through conduction velocities in 5-mo-old animals), so as to suppress overall conduction speed, just as we have found. A prediction of this model is that the conduction velocity in even older animals would eventually reach wild-type rates, as normal caliber is achieved throughout the length of the axons.

Our data reinforce a model (depicted schematically in Fig. 7 A) in which the key determinant(s) of radial growth are not mediated (solely) by the crossbridges provided by the extensively phosphorylated NF-H tails. Rather, linkages of the NF-M tail between filaments (Nakagawa et al., 1995) and longer-range interactions that rely upon additional putative linkers are likely to be central to structuring axoplasm. Possible candidates for such linkers within sensory axons include the plakin family of proteins such as BPAGn/dystonin, proposed as a crossbridging protein between neurofilaments and actin filaments (Yang et al., 1996) or microtubules (Yang et al., 1999). BPAG1n isoforms are essential for the postnatal survival of sensory neurons during the phase of rapid radial growth (Brown et al., 1995; Guo et al., 1995). Within motor axons, another cytoskeletal-linker protein is plectin and its isoforms (Rao et al., 1998) that carry binding sites for intermediate filaments, actin and microtubules (Wiche, 1989). This is an essential crosslinker in mice (Andra et al., 1997), and some isoforms of it are expressed in many neurons, including motor neurons (Errante et al., 1994). Indeed, linkers of both types (i.e., linear and the more complex forked pattern characteristic of plectin) are clearly seen in the quick-freeze deep-etch elec-

tron micrographs of the NF-H$^{tail\Delta}$ axons (Fig. 4 E). Additionally, gigaxonin, point mutations in which lead to large accumulations of neurofilaments within sensory axons thereby causing the disease giant axonal neuropathy (Bomont et al., 2000), has the potential to function as a linker in both motor and sensory axons. In the absence of the NF-H tail and its phosphorylation (Fig. 7 B), our evidence supports the view that the remaining linkers can assemble a flexible, deformable scaffold of interlinked cytoskeletal elements that supports axonal volume, albeit more slowly.

Materials and methods

Construction of NF-HTL mice by ES cell mediated knock in approach

A targeting vector was constructed with a genomic clone isolated from a mouse 129 SvJ library (Rao et al., 1998) by using PCR to introduce a Bsp H1 site after codon 475 of the NF-H protein. An in-frame Myc-tag sequence with translation stop and a segment specifying polyadenylation were ligated after Bsp HI digestion. A PGK-NEO cassette (Tybulewicz et al., 1991) was added along with a Bam HI-Eco RV (RV) fragment of NF-H gene as a 3′ arm for homologous recombination. The targeting vector was linearized with Sal I and electroporated into RI ES cells, provided by Dr. Andreas Nagy (University of Toronto, Toronto, Canada), and cells were selected for resistance to 200 μg/ml G418 and 2 μM gancyclovir. All cell manipulations were performed as described (Joyner, 1994). Drug resistant colonies were amplified, and DNA was prepared, digested with Hind III, separated on 0.8% agarose gels and transferred to Hybond N+ filters (Amersham Biosciences). Blots were hybridized with random primer labeled 0.5 kb Eco RI-Nde I or 1.4 kb Eco RV-Aat II probe fragments (Fig. 1 A).

Detection and quantification of neurofilament and tubulin proteins by immunoblotting

Sciatic and optic nerves extracts were made as described (Rao et al., 1998). Protein concentration was determined using bicinchoninic acid assay kit (Pierce Chemical Co.). Protein extracts, as well as known amounts of neurofilament standards, were separated on 7% polyacrylamide gels with SDS and transferred to nitrocellulose membranes (Lopata and Cleveland, 1987). The NF-H and NF-L subunits were identified using an affinity-purified rabbit polyclonal antibodies pAb-NF-H$_{COOH}$ and pAb-NF-L$_{COOH}$ raised against the COOH-terminal 12 amino acids of mouse NF-H and NF-L, respectively (Xu et al., 1993). The NF-H$^{tail\Delta}$ subunit was detected with an affinity-purified polyclonal Myc antibody (Gill et al., 1990), followed by ^{125}I-conjugated protein A. mAbs to NF-M (RMO44; Tu et al., 1995), α-tubulin (DM1A; Sigma-Aldrich), β-tubulin (18D6; Theodorakis and Cleveland, 1992), neuron-specific, class III β-tubulin (TuJ1; Lee et al., 1990), and intermediate filament antigen (IFA; Pruss et al., 1981) were used to identify each subunit, followed by goat anti–mouse IgG (Sigma-Aldrich) and ^{125}I-conjugated protein A. The immunoreactive bands were visualized by autoradiography and quantified by phosphorimaging (Molecular Dynamics) using known amounts of purified mouse spinal cord neurofilament standards.

Slow axonal transport studies in optic nerves

Retinal ganglion cells from NF-H$^{tail\Delta}$, NF-H deleted or their control littermate animals were radiolabeled in situ with 80 μCi of ^{35}S-methionine by intravitreal injection with a calibrated micropipette apparatus into anesthetized mice at 3 to 4 months of age (Nixon, 1980). 1 wk after injection, mice were sacrificed by cervical dislocation, and optic pathways were dissected. Three to four animals were analyzed for each genotype. The optic pathways were frozen and cut into nine consecutive segments of each 1.1 mm. Each was homogenized with a buffer containing 1% Triton X-100, 50 mM Tris, pH 6.8, 2 mM EDTA, 1 mM PMSF, and 50 μg/ml of protease inhibitor cocktail (Boehringer Mannheim). After centrifugation, the Triton insoluble cytoskeleton and soluble protein fractions were analyzed on 5–15% polyacrylamide gradient gels, transferred to nitrocellulose membranes and quantified by phosphorimaging.

Tissue preparation and morphological analysis

Mice were perfused transcardially with 4% paraformaldehyde, 2.5% glutaraldehyde in 0.1 M sodium cacodyalate buffer, pH 7.2, and postfixed overnight in the same buffer. Samples were treated with 2% osmium tetroxide, washed, dehydrated, and embedded in Epon-Araldite resin. Thick sections (0.75 μm) for light microscopy were stained with toluidine blue, and thin sections (70 nm) for electron microscopy were stained with uranyl acetate and lead acetate. Axons were counted in L5 root cross sections from three to four mice of each genotype and each age group. Axon diameters from five animals of each genotype and age were measured using the Bioquant Software. Entire roots were imaged, imaging thresholds were selected individually, and the cross sectional area of each axon was calculated and reported as a diameter of a circle of equivalent area. Axon diameters were grouped into 0.5-μm bins.

Visualization of neurofilament organization in the axon by quick-freeze deep-etch analysis

Sciatic nerves of 3- to 4-mo-old NF-H$^{tail\Delta}$, NF-H–deleted, and their control littermate animals were dissected and incubated in oxygenated artificial cerebrospinal fluid containing (in mM, pH 7.3): 126 NaCl, 22 $NaHCO_3$, 1 Na_2HPO4, 2.8 KCl, 0.88 $MgCl_2$, 1.45 $CaCl_2$, and 3.5 glucose. After sectioning with a razor blade, the tissue was frozen by slamming against a liquid helium-cooled copper block (E7200; Polaron) as previously reported (Gotow et al., 1999). The frozen tissue was mounted onto the freeze fracture apparatus (BAF 400D; Balzers), fractured, and then deep etched and rotary-replicated with platinum/carbon at an angle of 25°. The replicas were examined with a Hitachi H-300 electron microscope at 75kV.

Nerve conduction velocity measurements

Nerve conduction velocities were measured in the sciatic nerve, interosseus muscle system of 5-mo-old mice (Calcutt et al., 1990). Briefly, mice were anesthetized with halothane (4% in O_2 for induction, 2-3% for maintenance), and rectal temperature was maintained at 37°C by a heating lamp and thermal pad connected to a temperature regulator and the rectal thermistor probe. The sciatic nerve was stimulated with single supramaximal square wave pulses (4–8 V and 0.05 ms duration) via fine needle electrodes placed at the sciatic notch and Achilles tendon. Evoked electromyograms were recorded from the interosseus muscles of the ipsilateral foot via two fine needle electrodes and displayed on a digital storage oscilloscope. The distance between the two sites of stimulation was measured using calipers, and conduction velocity was calculated as described (Calcutt et al., 1990). Measurements were made in triplicate from a minimum of five animals for each genotype, and the median was used as the measure of velocity. Statistical ANOVA was done with a Bonferroni Multiple Comparisons Test post-hoc analysis using InStat.

We thank Janet Folmer and Asok Kumar for their help with electron microscopy, and Hayley McAuliff for help with manuscript preparation.

This work has been supported by grants R01 NS 27036 to D.W. Cleveland and National Institutes of Health/National Institute on Ageing AG0564 to R.A. Nixon. This work is also supported by the startup funds to M.V. Rao from the Center for Dementia Research at the Nathan Kline Institute. Salary support for D.W. Cleveland is provided by the Ludwig Institute for Cancer Research. M.L. Garcia was supported in part by a postdoctoral fellowship from the National Institutes of Health.

Submitted: 8 February 2002
Revised: 24 June 2002
Accepted: 25 June 2002

References

Andra, K., H. Lassmann, R. Bittner, S. Shorny, R. Fassler, F. Propst, and G. Wiche. 1997. Targeted inactivation of plectin reveals essential function in maintaining the integrity of skin, muscle, and heart cytoarchitecture. *Genes Dev.* 11:3134–3156.

Bass, P.W., and A. Brown. 1997. Slow axonal transport: the polymer transport model. *Trends Cell Biol.* 7:380–384.

Bernier, G., M. Pool, M. Kilcup, F. Alfoldi, Y-.E. Repentigny, and R. Kothary. 2000. Acf7 (MACF) is an actin and microtubule binding linker protein whose expression predominates in neural, muscle, and lung development. *Dev. Dyna.* 219:216–225.

Black, M.M., and R.J. Lasek. 1979. Axonal transport of actin: slow component b is the principal source of actin for axons. *Brain Res.* 171:401–423.

Black, M.M., and R.J. Lasek. 1980. Slow components of axonal transport: two cytoskeletal networks. *J. Cell Biol.* 86:616–623.

Bomont, P., L. Cavalier, F. Blondeau, C. Ben Hamida, S. Belal, M. Tazir, E. Demir, H. Topaloglu, R. Korinthenberg, B. Tuysuz, et al. 2000. The gene encoding gigaxonin, a new member of the cytoskeletal BTB/kelch repeat

family, is mutated in giant axonal neuropathy. *Nat. Genet.* 26:370–374.

Brady, S.T., and R.J. Lasek. 1981. Nerve specific enolase and creatine phosphokinase in axonal transport soluble proteins and the axoplasm matrix. *Cell.* 2:515–521.

Brown, A., G. Bernier, M. Mathieu, J. Rossant, and R. Kothary. 1995. The mouse dystonia musculorum gene is a neural isoforms of bullous pemphigoid antigen. *Nat. Genet.* 10:301–306.

Calcutt, N.A., D.R. Tomlinson, and S. Biswas. 1990. Coexistence of nerve conduction deficit with increased Na^+-K^+ ATPase activity in galactose-fed mice: implications for polyol pathway and diabetic neuropathy. *Diabetes.* 39:663–666.

Carden, M.J., W.W. Schlaepfer, and V.M.-Y. Lee. 1985. The structure, biochemical properties, and immunogenicity of neurofilament peripheral regions are determined by phosphorylation state. *J. Biol. Chem.* 260:9805–9817.

Chen, J., T. Nakata, Z. Zhang, and N. Hirokowa. 2000. The C-terminal tail domain of neurofilament protein-H (NF-H) forms the cross-bridges and regulates neurofilament bundle formation. *J. Cell Sci.* 113:3861–3869.

Ching, G.Y., and R.K. Liem. 1993. Assembly of type IV neuronal intermediate filaments in nonneuronal cells in the absence of preexisting cytoplasmic intermediate filaments. *J. Cell Biol.* 122:1323–1335.

Collard, J.F., F. Cote, and J.-P. Julien. 1995. Defective axonal transport in a transgenic mouse model of amyotrophic lateral sclerosis. *Nature.* 375:614–618.

Cote, F., J.F. Collard, and J.P. Julien. 1993. Progressive neuronopathy in transgenic mice expressing the human neurofilament heavy gene: a mouse model of amyotrophic lateral sclerosis. *Cell.* 73:35–46.

Dalpe, G., N. Leclerc, A. Vallee, A. Messer, M. Mattrieu, Y.-D. Repentigny, and R. Kothary. 1998. Dystonin is essential for maintaining neuronal cytoskeletal organization. *Mol. Cell. Neurosci.* 10:243–247.

de Waegh, A.M., V.M.-Y. Lee, and S.T. Brady. 1992. Local modulation of neurofilament phosphorylation, axonal caliber, and slow axonal transport by myelinating Schwann cells. *Cell.* 68:451–453.

Elder, G.A., V.L. Fredric, Jr., C. Kang, P. Basco, A. Gourav, P.-H. Tu, V.M.-Y. Lee, and R.A. Lazzarini. 1998a. Absence of mid-sized neurofilament subunit decreases axonal caliber, levels of neurofilament (NF-L), and neurofilament content. *J. Cell Biol.* 141:727–739.

Elder, G.A., V.L. Fiedrich, Jr., C. Kang, P. Basco, A. Gourav, P.-H. Tu, B. Zhang, V.M.-Y. Lee, and R.A. Lazzarini. 1998b. Requirement of heavy neurofilament subunit in the development of axons with large calibers. *J. Cell Biol.* 143:195–205.

Errante, L.D., G. Wiche, and G. Shaw. 1994. Distribution of plectin, an intermediate filament associated protein, in the adult rat central nervous system. *J. Neurosci. Res.* 37:515–528.

Eyer, J., and A. Peterson. 1994. Neurofilament deficient axons and perikaryal aggregates in viable transgenic mice expressing a neurofilament-β-galactosidase fusion protein. *Neuron.* 12:389–405.

Friede, R.L., and T. Samorajski. 1970. Axon caliber related to neurofilaments and microtubules in sciatic nerve fibers of rats and mice. *Anat. Rec.* 176:379–387.

Garner, J., and R.J. Lasek. 1981. Clathrin is axonally transported as part of slow component b: the microfilament complex. *J. Cell Biol.* 88:172–178.

Gasser, H.S., and H. Grundfest. 1939. Axon diameters in relations to the spike dimensions and the conduction velocity in mammalian A fibers. *Am. J. Physiol.* 127:393–414.

Geisler, N., E. Kaufmann, S. Fischer, U. Plessmann, and K. Weber. 1983. Neurofilament architecture combines structural principles of intermediate filaments with carboxyl-terminal extensions increasing in size between triplet proteins. *EMBO J.* 2:1295–1302.

Geisler, N., J. Vandekerckhove, and K. Weber. 1987. Location and sequence characterization of the major phosphorylation sites of the high molecular mass neurofilament proteins M and H. *FEBS Lett.* 221:403–407.

Gill, S.R., P.C. Wong, M.J. Monterio, and D.W. Cleveland. 1990. Assembly properties of dominant and recessive mutations in the small mouse neurofilament (NF-L) subunit. *J. Cell Biol.* 111:2005–2019.

Glicksman, M.A., D. Soppet, and M.B. Willard. 1987. Posttranslational modifications of neurofilament polypeptides in rabbit retina. *J. Neurobiol.* 18:167–196.

Goldstein, M.E., L.A. Sternberger, and N.H. Sternberger. 1987. Varying degrees of phosphorylation determine microheterogeneity of the heavy neurofilament polypeptide (NF-H). *J. Neuroimmunol.* 14:135–148.

Gotow, T., J.F. Leterrier, Y. Ohsawa, T. Watanabae, K. Isahara, R. Shibata, K. Ikenaka, and Y. Uchiyama. 1999. Abnormal expression of neurofilament proteins in dysmyelinating axons located in the central nervous system of jimpy mutant mice. *Eur. J. Neurosci.* 11:3983–3903.

Guo, L., L. Degenstein, J. Dowling, Q.C. Yu, R. Wollmann, B. Perman, and E. Fuchs. 1995. Gene targeting of BPAG1: abnormalities in mechanical strength and cell migration in stratified epithelia and neurologic degeneration. *Cell* 81:233-43.

Hirokawa, N., S. Terada, T. Funmakoshi, and S. Terada. 1997. The slow axonal transport: the subunit model. *Trends Cell Biol.* 7:384–388.

Hisanaga, S., and N. Hirokawa. 1990. Dephosphorylation-induced interaction of neurofilaments with microtubules. *J. Biol. Chem.* 265:21852–21858.

Hisanaga, S., M. Kusubata, E. Okumura, and T. Kishimoto. 1991. Phosphorylation of neurofilament H subunit at the tail domain by CDC2 kinase dissociates the association to microtubules. *J. Biol. Chem.* 266:21793–21803.

Hoffman, P.N., and R.J. Lasek. 1975. The slow component of axonal transport: identification of major structural polypeptides of the axon and their generality among mammalian neurons. *J. Cell Biol.* 66:351–366.

Hoffman, P.N., D.W. Cleveland, J.W. Griffin, P.W. Landes, N.J. Cowan, and D.L. Price. 1987. Neurofilament gene expression: a major determinant of axonal caliber. *Proc. Natl. Acad. Sci. USA.* 84:3472–3476.

Hsieh, S.-T., G.J. Kidd, T.O. Crawford, Z-.S. Xu, B.D. Trapp, D.W. Cleveland, and J.W. Griffin. 1994. Regional modulation of neurofilament organization by myelination in normal axons. *J. Neurosci.* 14:6392–6401.

Jacomy, H., Q. Zhu, S. Couillard-Despres, J.-M. Beaulieu, and J.-P. Julien. 1999. Disruption of type IV intermediate filament network in mice lacking the neurofilament medium and heavy subunits. *J. Neurochem.* 73:972–984.

Jones, S.M., and R.C. Williams. 1982. Phosphate content of mammalian neurofilaments. *J. Biol. Chem.* 256:9902–9905.

Joyner, A.L. 1994. Gene Targeting. A Practical Approach. IRL Press, New York. 234 pp.

Julien, J.-P., and W.E. Mushynski. 1982. Multiple phosphorylation sites in mammalian neurofilament polypeptides. *J. Biol. Chem.* 257:10467–10470.

Julien, J.-P., and W.E. Mushynski. 1983. The distribution of phosphorylation sites among identified proteolytic fragments of mammalian neurofilaments. *J. Biol. Chem.* 258:4019–4025.

Jung, C., J.T. Yabe, S. Lee, and T.B. Shea. 2000a. Hypophosphorylated neurofilament subunits undergo axonal transport more rapidly than more extensively phosphorylated subunits in situ. *Cell Motil. Cytoskeleton.* 47:120–129.

Jung, C., J.T. Yabe, and T.B. Shea. 2000b. C-terminal phosphorylation of the high molecular weight neurofilament subunit correlates with decreased neurofilament axonal transport velocity. *Brain Res.* 856:12–19.

Kriz, J., Q. Zhu, J.-P. Julien, and A.L. Padjen. 2000. Electrophysiological properties of axons in mice lacking neurofilament subunit genes: disparity between conduction velocity and axon diameter in absence of NF-H. *Brain Res.* 885:32–44.

Lee, V.M.-Y., M.J. Carden, and J.Q. Trojonowski. 1986. Novel monoclonal antibodies provide evidence for the in situ existence of a nonphosphorylated form of the largest neurofilament subunit. *J. Neurosci.* 6:850–858.

Lee, V.M.-Y., L. Otvos, Jr., M.J. Carden, M. Hollosi, B. Dietzschold, and R.A. Lazzarini. 1988. Identification of the major multiphosphorylation site in mammalian neurofilaments. *Porc. Natl. Acad. Sci. USA.* 85:1998–2002.

Lee, M.K., J.B. Tuttle, L.I. Rebhum, D.W. Cleveland, and A. Frankfurter. 1990. The expression and posttranslational modification of a neuron-specific β-tubulin isotype during chick embryogenesis. *Cell Motil. Cytoskeleton.* 17:118–132.

Lee, M.K., Z. Xu, P.C. Wong, and D.W. Cleveland. 1993. Neurofilaments are obligate heteropolymers in vivo. *J. Cell Biol.* 122:1337–1350.

Leung, C.L., D. Sun, M. Zheng, D.R. Knowles, and R.K. Leim. 1999. Microtubule actin cross-linking factor (MACF): a hybrid of dystonin-dystrophin that can interact with the actin and microtubule cytoskeleton. *J. Cell Biol.* 147:1275–1286.

Leung, C.L., M. Zheng, S.M. Prater, and R.K.H. Liem. 2001. The BPAG1 locus: alternative splicing produces multiple isoforms with distinct cytoskeletal linker domains, including predominant isoforms in neurons and muscles. *J. Cell Biol.* 154:691–697.

Lewis, S.E., and R.A. Nixon. 1988. Multiple phosphorylated variants of high molecular weight subunit of neurofilaments of retinal cell neurons: characterization and evidence for their differential association with stationary and moving neurofilaments. *J. Cell Biol.* 107:2689–2701.

Lopata, M.A., and D.W. Cleveland. 1987. In vivo microtubules are copolymers of available β-tubulin isotypes: localization of each of six vertebrate β-tubulin isotypes using polyclonal antibodies elicited by synthetic peptide antigens. *J. Cell Biol.* 105:1707–1720.

Marszalek, J.R., T.L. Williamson, M.K. Lee, Z.- S. Xu, T.O. Crawford, P.N. Hoffman, and D.W. Cleveland. 1996. Neurofilament subunit H modulates axonal diameter by affecting the rate of neurofilament transport. *J. Cell Biol.* 135:711–724.

Meier, J., S. Couillard-Despres, H. Jacomy, C. Gravel, and J.P. Julien. 1999. Extra neurofilament NF-L subunits rescue motor neuron disease caused by overex-

pression of the human NF-H gene in mice. *J. Neuropathol. Exp. Neurol.* 58: 1099–1110.

Miyasaka, H., S. Okabe, K. Ishiguro, T. Uchida, and N. Hirokawa. 1993. Interaction of the tail domain of high molecular weight subunits of neurofilaments with the COOH-terminal region of tubulin and its regulation by τ protein kinase II. *J. Biol. Chem.* 268:22695–22702.

Monteiro, M.J., P.N. Hoffman, J.D. Gearhart, and D.W. Cleveland. 1990. Expression of NF-L in both neuronal and nonneuronal cells of transgenic mice: increased neurofilament density without affecting the caliber. *J. Cell Biol.* 111:1543–1557.

Nakagawa, T., J. Chen, Z. Zhang, Y. Kanai, and N. Hirokawa. 1995. Two distinct functions of the carboxyl-terminal tail domain of NF-M upon neurofilament assembly: cross-bridge formation and longitudinal elongation of filaments. *J. Cell Biol.* 129:411–429.

Nixon, R.A. 1980. Protein degradation in mouse visual system. I. Degradation of axonally transported and retinal proteins. *Brain Res.* 200:69–83.

Nixon, R.A. 1993. The regulation of neurofilament protein dynamics by phosphorylation: clues to neurofibrillary pathobiology. *Brain Pathol.* 3:29–38.

Nixon, R.A., and S.E. Lewis. 1986. Differential turnover of phosphate groups on neurofilament subunits in mammalian neurons *in vivo*. *J. Biol. Chem.* 261: 16298–16301.

Nixon, R.A., and R.K. Sihag. 1991. Neurofilament phosphorylation: a new look at regulation and function. *Trends Neurosci.* 14:501–506.

Nixon, R.A., B.A. Brown, and C.A. Morotta. 1982. Posttranslational modification of a neurofilament protein during axoplasmic transport: implications for regional specialization of CNS axons. *J. Cell Biol.* 94:150–158.

Nixon, R.A., S.E. Lewis, and C.A. Morota. 1987. Posttranslational modification of neurofilament proteins by phosphate during axoplasmic transport in retinal ganglion cell neurons. *J. Neurosci.* 7:1145–1158.

Nixon, R.A., I. Fischer, and S.E. Lewis. 1990. Synthesis, axonal transport, and turnover of the high molecular weight microtubule-associated protein MAP1A in mouse retinal ganglion cells: tubulin and MAP1A display distinct transport kinetics. *J. Cell Biol.* 110:437–448.

Nixon, R.A., P.A. Paskevich, R.K. Sihag, and C.Y. Thayer. 1994. Phosphorylation on carboxyl terminus domains of neurofilament proteins in retinal ganglion cell neurons in vivo: influences on regional neurofilament accumulation, interfilament spacing and axonal caliber. *J. Cell Biol.* 126:1031–1046.

Oblinger, M.M., S.T. Brady, I.G. McQuarrie, and R.J. Lasek. 1987. Cytotypic differences in the protein composition of the axonally transported cytoskeleton in mammalian neurons. *J. Neurosci.* 7:453–462.

Ohara, O., Y. Gahara, T. Miyake, H. Teraoka, and T. Kitamura. 1993. Neurofilament deficiency in quail caused by nonsense mutation in neurofilament-L gene. *J. Cell Biol.* 121:387–395.

Prahlad, V., B.T. Helfand, G.M. Longford, R.D. Vale, and R.D. Goldman. 2000. Fast transport of neurofilament protein along microtubules in squid axoplasm. *J. Cell Sci.* 113:3939–3946.

Pruss, R.M., R. Mirsky, and M. Raff. 1981. All classes of intermediate filaments share a common antigenic determinant defined by a monoclonal antibody. *Cell.* 27:419–428.

Rao, M.V., M.K. Houseweart, T.L. Williamson, T.O. Crawford, J. Folmer, and D.W. Cleveland. 1998. Neurofilament dependent radial growth of motor axons and axonal organization of neurofilaments does not require the neurofilament heavy subunit (NF-H) or its phosphorylation. *J. Cell Biol.* 143: 171–181.

Roy, S., P. Coffee, G. Smith, R.K.H. Liem, S.T. Brady, and M.M. Black. 2000. Neurofilaments are transported rapidly but intermittently in axons: implications for slow axonal transport. *J. Neurosci.* 20:6849–6861.

Rushton, W.A.H. 1951. A theory of the effects of fiber size in medullated nerve. *J. Physiol.* 115:101–122.

Sanchez, I., L. Hassinger, P.A. Paskevich, H.D. Shine, and R.A. Nixon. 1996. Oligodendroglia regulate the regional expansion of axon caliber and local accumulation of neurofilaments during development independently of myelin formation. *J. Neurosci.* 16:5095–5105.

Sanchez, I., L. Hassinger, R.K. Sihag, D.W. Cleveland, P. Mohan, and R.A. Nixon. 2000. Local control of neurofilament accumulation during radial growth of myelinating axons in vivo: selective role of site-specific phosphorylation. *J. Cell Biol.* 151:1013–1024.

Shah, J.V., and D.W. Cleveland. 2002. Slow axonal transport: fast motors in slow lane. *Curr. Opin. Cell Biol.* 14:58–62.

Shah, J.V., L.A. Flanagan, P.A. Janemy, and J.F. Leterrier. 2000. Bidirectional translocation of neurofilaments along microtubules mediated in part by dynein/dynactin. *Mol. Biol. Cell.* 11:3495–3508.

Sihag, R.K., and R.A. Nixon. 1991. Identification of Ser-55 as a major protein kinase A phosphorylation site on the 70-kDa subunit of neurofilaments: early turnover during axonal transport. *J. Biol. Chem.* 266:18861–18867.

Sternberger, L.A., and N.H. Sternberger. 1983. Monoclonal antibodies distinguish phosphorylated and nonphosphorylated form of neurofilaments *in situ*. *Proc. Natl. Acad. Sci. USA.* 80:6126–6130.

Svitkina, T.M., A.B. Verkhovsky, and G.G. Borisy. 1996. Plectin side arms mediate interaction of intermediate filaments with microtubules and other components of cytoskeleton. *J. Cell Biol.* 135:991–1007.

Terada, S., T. Nakata, A.C. Peterson, and N. Hirokawa. 1996. Visualization of slow axonal transport in vivo. *Science.* 273:784–788.

Theodorakis, N.G., and D.W. Cleveland. 1992. Physical evidence for the cotranslational regulation of beta-tubulin m-RNA degradation. *Mol. Cell. Biol.* 12: 791–799.

Tu, P.-H., G. Elder, R.A. Lazzarini, D. Nelson, J.Q. Trojanowski, and V.M. Lee. 1995. Overexpression of human NF-M subunit in transgenic mice modifies the level of endogenous NF-L and the phosphorylation state of NF-H subunits. *J. Cell Biol.* 129:1629–1640.

Tybulewicz, V.L., J.C.E. Crawford, P.K. Jackson, R.T. Bronson, and R.C. Mulligan. 1991. Neonatal lethality and lymphopenia in mice with a homozygous disruption of the c-abl proto-oncogene. *Cell.* 65:1153–1163.

Wang, L., C.-I. Ho, D. Sun, R.K.H. Liem, and A. Brown. 2000. Rapid movement of axonal neurofilaments interrupted by prolonged pauses. *Nat. Cell Biol.* 2:137–141.

Waxman, S.G. 1980. Determinants of conduction velocity in myelinated nerve fibers. *Muscle Nerve.* 3:141–150.

Wiche, G. 1989. Plectin: general overview and appraisal of its potential role as a subunit protein of the cytomatrix. *Crit. Rev. Biochem. Mol. Biol.* 24:41–67.

Willard, M. 1977. The identification of two intra-axonally transported polypeptides resembling myosin in some respects in the rabbit visual system. *J. Cell Biol.* 75:1–11.

Willard, M., and C. Simon. 1983. Modulation of neurofilament axonal transport during the development of rabbit retinal ganglion cells. *Cell.* 35:551–559.

Willard, M., M. Wiseman, J. Levine, and P. Skene. 1979. Axonal transport of actin in rabbit retinal ganglion cells. *J. Cell Biol.* 81:581–591.

Wong, P.C., J. Marszalek, T.O. Crawford, Z. Xu, S.T. Hsieh, J.W. Griffin, and D.W. Cleveland. 1996. Increaseing neurofilament subunit M expression reduces axonal NF-H, inhibits radial growth, and results in neurofilamentous accumulation in motor neurons. *J. Cell Biol.* 130:1413–1422.

Xu, Z., L.C. Cork, J.W. Griffin, and D.W. Cleveland. 1993. Increased expression of neurofilament subunit L produces morphological alterations that resemble the pathology of human motor neuron disease. *Cell.* 73:23–33.

Xu, Z.-S., J.R. Marszalek, M.K. Lee, P.C. Wong, J. Folmer, T.O. Crawford, S.-T. Hsieh, J.W. Griffin, and D.W. Cleveland. 1996. Subunit composition of neurofilaments specifies axonal diameter. *J. Cell Biol.* 133:1061–1069.

Yabe, J.T., A. Pimenta, and T.B. Shea. 1999. Kinesin-mediated transport of neurofilament protein oligomers in growing axons. *J. Cell Sci.* 112:3799–3814.

Yabe, J.T., T. Chylinski, F.-S. Wang, A. Pimenta, S.D. Kattar, M.-D. Linsley, W.K.-H. Chan, and T.B. Shea. 2001. Neurofilaments consist of distinct populations that can be distinguished by C-terminal phosphorylation, bundling, and axonal transport rate in growing axonal neuritis. *J. Neurosci.* 21: 2195–2205.

Yang, Y., J. Dowling, Q.C. Yu, P. Kouklis, D.W. Cleveland, and E. Fuchs. 1996. An essential cytoskeletal linker protein connecting actin microfilaments to intermediate filaments. *Cell.* 86:655–665.

Yang, Y., C. Bauer, G. Strasser, R. Wollman, J.P. Julien, and E. Fuchs. 1999. Integrators of the cytoskeleton that stabilize the microtubules. *Cell.* 98:229–238.

Yin, X., T.O. Crawford, J.W. Griffin, P.H. Tu, V.M.-Y. Lee, C. Li, R. Roder, and B.D. Trapp. 1998. Myelin-associated glycoprotein is a myelin signal that modulates the caliber of myelinated axons. *J. Neurosci.* 18:1953–1962.

Zhu, Q., S. Couillard-Despres, and J.-P. Julien. 1997. Delayed maturation of regenerating myelinated axons in mice lacking neurofilaments. *Exp. Neurol.* 148:299–316.

Zhu, Q., M. Lindenbaum, F. Levavasseur, H. Jacomy, and J.-P. Julien. 1998. Disruption of the NF-H gene increases axonal microtubule content and velocity of neurofilament transport: relief of axonopathy resulting from the toxin beta, beta′-iminodipropionitrile. *J. Cell Biol.* 143:183–193.